Enhanced Born charges in III-VII, IV-VII_2, and V-VII_3 compounds

Mao-Hua Du and David J. Singh
Materials Science and Technology Division and Center for Radiation Detection Materials and Systems, Oak Ridge National Laboratory, Oak Ridge, Tennessee 37831, USA
(Received 8 June 2010; published 16 July 2010)

We report electronic-structure and lattice dynamics calculations on selected III-VII, IV-VII_2, and V-VII_3 compounds. The common characteristic of these largely ionic compounds is that their outmost cation-*s* states are fully occupied and thus the conduction-band states are derived from the more spatially extended cation-*p* states, resulting in significant cross-band-gap hybridization, which enhances Born effective charges substantially. The large Born charges cause large splitting between longitudinal and transverse optic phonon modes and large static dielectric constants resulting mostly from the lattice contribution. This can lead to effective screening of defects and impurities that would otherwise be strong carrier traps and recombination centers and may therefore have positive effects on the carrier transport properties in radiation detectors based on these soft-lattice halides.

DOI: 10.1103/PhysRevB.82.045203 PACS number(s): 71.20.Nr, 63.20.dk, 77.22.Ch

I. INTRODUCTION

Group III, IV, and V cations can form many compounds with group VI or VII anions. These cations have both *s* and *p* orbitals in their outmost valence shells, e.g., In has two 5*s* and one 5*p* valence electrons; Pb has two 6*s* and two 6*p* valence electrons, etc. Depending on whether the *s* orbitals are occupied or not, these group III, IV, and V cations can assume multiple oxidation states. For examples, the oxidation states for In are +1 in InI and +3 in InI_3 while different In in In_2I_4 have valences of +1 and +3. We are interested in the compounds with group III, IV, and V cations, whose outmost *s* orbitals are fully occupied, such as in InI, PbI_2, and BiI_3. Within the occupied valence bands, the lower-lying cation-*s* bands hybridize strongly with the higher-lying anion-*p* bands, leading to some peculiar electronic properties, such as abnormal band-gap order and valence-band offset in lead chalcogenides,[1] negative deformation potential in both lead chalcogenides[1] and thallium halides.[2] More recently, we have shown enhanced Born effective charges in thallium halides, leading to large splitting between longitudinal and transverse optical phonons (LO and TO) and proximity to ferroelectricity.[3] The large lattice polarization in thallium halides results in large static dielectric constants resulting mostly from the lattice contribution.

In this paper, we will generalize our findings in thallium halides to indium halides, lead halides, and bismuth halides. The filling of the cation-*s* band results in the unusual cation-*p* character of the conduction band, which is more delocalized than the conduction band states of many conventional semiconductors, typically of cation-*s* character if no transition metal ions are involved. We will show that the stronger cross-band-gap hybridization between the cation-*p* and anion-*p* bands in these largely ionic halides is responsible for the enhanced Born effective charges[4] and large LO-TO splitting, in consistence with the experimentally observed larger static dielectric constants. The cation-*p* character of the conduction band states can also be found in IV-VI and V_2-VI_3 compounds, many of which have large LO-TO splitting. Here we will focus on halides due to their large band gaps and potential applications in room-temperature radiation detection. The large static dielectric constants (due to the large lattice polarization) in these halides reduce the carrier trapping at impurities and defects, thereby improving the carrier transport properties. These may play a key role in radiation detection applications.

Room-temperature radiation detection requires high density, i.e., composition with large atomic number elements, for efficient radiation absorption, relatively large band gap (>1.4 eV) for room-temperature applications, high resistivity for suppressing dark current and device noise, and large $\mu\tau$ product (where μ and τ are carrier mobility and lifetime, respectively). Some halides considered in this study (InI, PbI_2, and BiI_3) have large atomic numbers, large enough band gap, high resistivity, and large static dielectric constants. This combination is desired for the room-temperature radiation detection applications. There has been considerable interest in investigating InI, PbI_2, and BiI_3 for potential applications in x-ray and γ-ray detection.[5–11]

II. METHODS

We performed density-functional calculations to study the electronic structure and lattice dynamics of III-VII, IV-VII_2, and V-VII_3 compounds. The electronic structures were calculated using projector-augumented wave method, as implemented in the plane-wave-based VASP package.[12] The Born effective charges were calculated using linear response in the VASP code and the phonon dispersion for InI was calculated using the QUANTUM ESPRESSO code[13] with norm-conserving pseudopotentials. Perdew-Burke-Ernzerhof exchange-correlation functionals[14] were used in all calculations.

III. RESULTS

A. Indium halides

InI and InBr crystallize in a base-centered orthorhombic TlI structure (space group 63).[15,16] The TlI structure is also a high-temperature phase (>390 K) for InCl.[17] These compounds have layered structures with every In atom bonded to

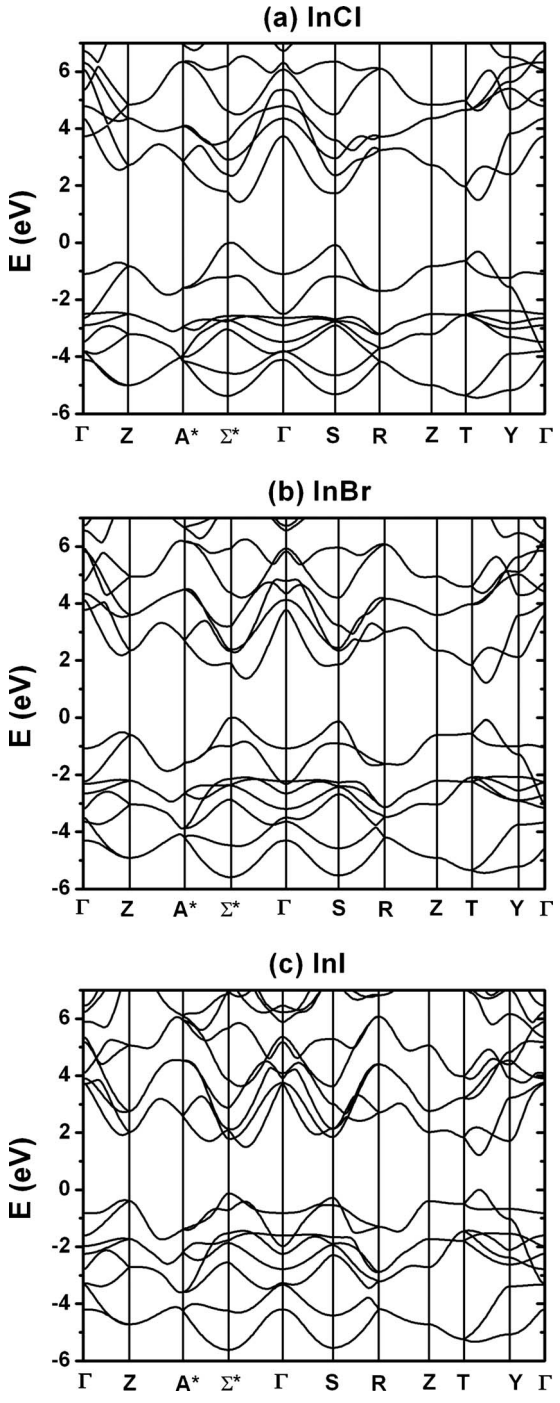

FIG. 1. Band structures of (a) InCl, (b) InBr, and (c) InI.

five halogen atoms within the layer and to two other In atoms in the adjacent layer. The band structures of InCl, InBr, and InI are shown in Fig. 1. The experimental lattice parameters were used in these calculations, i.e., a=4.242 Å, b =12.32 Å, and c=4.689 Å (InCl);[17] a=4.242 Å, b =12.32 Å, c=4.689 Å (InBr);[15] a=4.763 Å, b=12.781 Å, c=4.909 Å (InI).[16] As shown in Fig. 1(c), InI has a direct band gap on the H line (between T and Y points), which disagrees with previous calculations that show an indirect band gap.[18,19] On the other hand, indirect band gaps can be seen for InBr and InCl in Figs. 1(b) and 1(a). The valence-band maxima (VBM) for InBr and InCl are both at the Σ^* point while the conduction-band minima (CBM) are on the H line for InBr and on the Σ line (between Σ^* and Γ points) for InCl. Our results agree with the optical measurements that show direct band gap for InI and indirect band gap for InBr.[20] The calculated band gaps are 1.22 eV (InI), 1.22 eV (InBr), and 1.44 eV (InCl), compared to the measured band gaps of 2.02 eV (InI) (Ref. 21) and 2.13 eV (InBr).[22] The underestimation of the calculated band gaps is the common problem for the density-functional calculations.

As can be seen from Fig. 1, the band structures of the three indium halides are quite similar. The bands between −6 to −4 eV with respective to VBM are mostly derived from the In 5s states while the bands between −4 to 0 eV have mostly halogen p character. There is strong hybridization between the In 5s and halogen p states as shown by the projected density of states (DOS) shown in Fig. 2. Such hybridization is enhanced when the halogen changes from I to Br and Cl, as evidenced by the increasing In s component in the DOS near the VBM (see Fig. 2). This causes small change in band gaps going from InI to InBr and InCl since the lowering of the outmost p bands of the more electronegative halogen is largely prevented by the repulsion from the In 5s bands. The valence band maxima at the Σ^* and S points and on the H line are close in energy in indium halides. Their relative positions are sensitive to the symmetry-dependent hybridization between the In 5s and halogen p bands.

Significant cross-band-gap hybridization between the In p and halogen p states can also be seen in Fig. 2, suggesting some covalent character in these largely ionic compounds. The presence of covalent character in the mostly ionic bonding network has important consequences in lattice dynamics because the displacement of the positive charge center will cause the electron transfer in the opposite direction.[4] This effect enhances the lattice polarization, as has been discussed in ferroelectric oxides, such as $PbTiO_3$.[4,23–25] We will demonstrate below that the same mechanism also gives rise to large Born effective charges and large LO-TO splitting in these indium halides.

Figure 3 shows the phonon dispersions for InI. The phonon energy scale is low, with a maximum frequency just over 100 cm^{-1}, consistent with InI's soft lattice as evidenced by its low melting temperature of 360 °C. Since the crystal is biaxial, three LO and three TO modes are identified corresponding to three principal crystallographic axes. The three calculated LO modes are 99.7 (along a axis), 102.7 (b axis), and 92.6 (c axis) cm^{-1}, and the three calculated TO modes are 50.5 (a axis), 56.4 (b axis), and 40.8 (c axis) cm^{-1}. Infrared[26] (IR) and resonant Raman scattering[27] experiments reported LO modes of 106 and 111 cm^{-1}, respectively. The IR measurements also show a TO mode of 58 cm^{-1}.[26] However, the phonon anisotropy has not been resolved experimentally. Besides the three IR active optical phonon modes, there are six Raman modes, which are calculated to be 22.9, 34.2, 50.4, 62.2, 66.0, and 81.5 cm^{-1}, compared well to the measured Raman modes of 26.6, 42.8, 57.1, 68.3, 72.3, 86.7 cm^{-1}.[26] The large LO-TO splitting results from large Born effective charges, which measure how lattice polarization develops with atomic displacement. The calculated Born effective charges for In and I ions (see Table I) are nearly 2.5

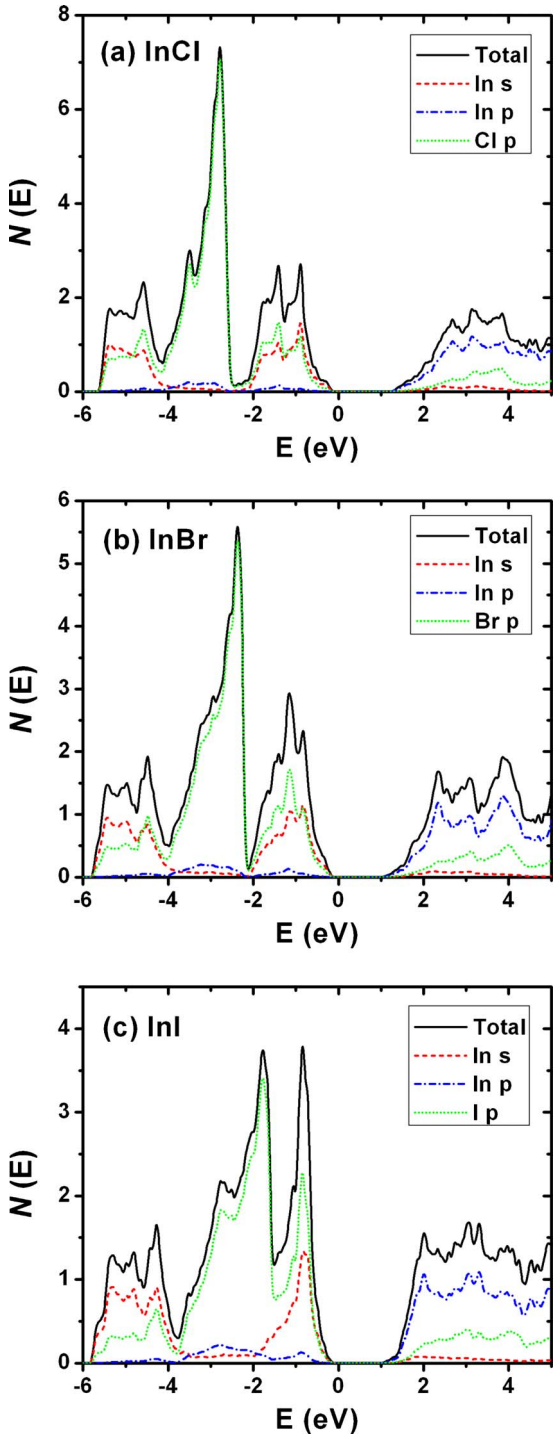

FIG. 2. (Color online) Projected density of states for (a) InCl, (b) InBr, and (c) InI. Note the cross-band-gap hybridization between the halogen p bands and the nominally unoccupied In $5p$ bands.

times larger than their nominal ionic charges (In: +1 and I: −1). This is due to the cross-band-gap hybridization between the I p and the spatially extended In p states (as can be seen in Fig. 2). Similarly, the calculated Born effective charges for InBr and InCl are also substantially larger than their nominal ionic charges as shown in Table I. The anomalously large Born effective charges reflect significantly enhanced dynamic coupling between atomic displacement and polarization.

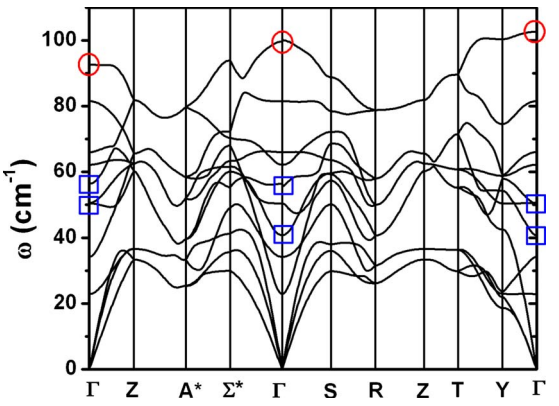

FIG. 3. (Color online) Phonon dispersion for InI. LO and TO phonons are indicated by red circles and blue squares, respectively.

The calculated large Born charges for indium halides should correspond to large lattice polarization and hence large static dielectric constants. The calculated high-frequency dielectric constants are $\varepsilon_\infty^{xx}=8.5$, $\varepsilon_\infty^{yy}=9.1$, $\varepsilon_\infty^{zz}=10.0$ (InI) and $\varepsilon_\infty^{xx}=6.5$, $\varepsilon_\infty^{yy}=7.4$, $\varepsilon_\infty^{zz}=8.1$ (InBr). These numbers may be overestimated due to the artificially small band gap from the calculation. The isotropic high-frequency (ε_∞) and static (ε_0) dielectric constants have been deduced as 7.7 and 25.7, respectively, for InI, and 6.5 and 34.7, respectively, for InBr, from the analysis of the IR reflection spectra by Clayman *et al.*[26] Clearly, the lattice contribution outweighs the electronic part by a substantial amount in the static dielectric constants of InI and InBr, consistent with our results of large Born charges and large LO-TO splittings.

B. PbI_2 and BiI_3

Similar to the III-VII compounds discussed above and in our previous publication on Tl halides,[3] IV-VII$_2$ and V-VII$_3$ compounds also have their outmost cation-s states fully occupied. Thus, their conduction-band states are derived from spatially more extended cation-p orbitals, leading to signifi-

TABLE I. Born effective charges (Z^*) for InI, InBr, InCl, PbI_2, and BiI_3. Note the nominal ionic charges are +1 for In, +2 for Pb, +3 for Bi, and −1 for all halogens. The Born charge for I in BiI_3 is not shown. It is a tensor involving nondiagonal elements.

Wave-vector direction	a	b	c
Z^* (InI)	2.4 (In)	2.5 (In)	2.5 (In)
	−2.4 (I)	−2.5 (I)	−2.5 (I)
Z^* (InBr)	2.1 (In)	2.4 (In)	2.4 (In)
	−2.1 (Br)	−2.4 (Br)	−2.4 (Br)
Z^* (InCl)	1.8 (In)	2.3 (In)	2.2 (In)
	−1.8 (Cl)	−2.3 (Cl)	−2.2 (Cl)
Z^* (PbI_2)	4.0 (Pb)	4.0 (Pb)	1.92 (Pb)
	−2.0 (I)	−2.0 (I)	−0.96 (I)
Z^* (BiI_3)	5.2 (Bi)	5.2 (Bi)	2.8 (Bi)

cant cross-band-gap hybridization and enhanced Born effective charges. Here we will discuss two representative IV-VI_2 and V-VI_3 compounds, i.e., PbI_2 and BiI_3, both of which are promising x-ray and γ-ray detectors.

PbI_2 crystallizes in a hexagonal CdI_2 structure (space group 164) with lattice constants: a=4.5580, b=4.5580, and c=6.986 Å.[28] BiI_3 crystallizes in a rhombohedral structure (space group 148) with lattice constants: a=7.516, b=7.516, and c=20.72 Å.[29] Both compounds have layered structure with significant anisotropy between the directions parallel and perpendicular to the c axis. We have calculated the Born charges in these two iodides using their experimental lattice constants. As shown in Table I, abnormally large Born charges in the ab plane are found, while the Born charges along the c axis are normal, close to their nominal ionic charges. These results suggest that there is enhanced in-plane lattice polarization that should be substantially larger than the out-of-plane lattice polarization. The measurements of IR reflectivity spectra show that, for PbI_2, there is an in-plane static dielectric constant ε_0 ($\mathbf{E}\perp c$)=26.4 (lattice contribution is 20.3),[30] much larger than the out-of-plane ε_0 ($\mathbf{E}\| c$) =6.5.[31] Similarly, very large difference between the in-plane and out-of-plane static dielectric constants for BiI_3 [ε_0 ($\mathbf{E}\perp c$)=54, ε_0 ($\mathbf{E}\| c$)=8.6] has been reported.[32] Again, the lattice contribution dominates the in-plane dielectric constant since the high-frequency dielectric constants are small, i.e., ε_∞ ($\mathbf{E}\perp c$)=7.1, ε_∞ ($\mathbf{E}\| c$)=6.4.[33] These experimental results are consistent with our calculated large Born effective charges for PbI_2 and BiI_3.

IV. DISCUSSION

As discussed above, the enhanced Born charges as a result of the cross-band-gap hybridization in the largely ionic halides studied in this paper may be related to the delocalized cation-p character of the CBM states. To gain more insight, we have also calculated Born charges for HgI_2, which has the normal cation-s character for the conduction band. The calculated Born charges for Hg are +2.8 (in-plane) and +2.3 (out-of-plane), compared to the nominal ionic charge of +2. Apparently, the enhancement of Born charges for HgI_2 is much smaller than the typical enhancement found in the III-VII, IV-VII_2, and V-VII_3 compounds as shown in Table I. As a result, the static dielectric constant for HgI_2 is only 8.8.[34]

Similar Born charge enhancement has been found in many ferroelectric oxides. In general, ferroelectricity is governed by a balance between the long-range Coulomb interactions and the short-range close-shell repulsion between ions. The former favors ferroelectricity while the latter does not. In oxides, the divalent anions have twice the nominal charge of halogen ions and therefore on average the cations have twice larger charges as well. This leads to larger Coulomb interactions. Thus, in oxides, ferroelectricity is often seen, while the halides are rarely ferroelectric, but nonetheless as discussed above can have enhanced Born charges leading to useful enhancement of the dielectric screening.

Ionic and soft-lattice compounds often have inferior transport properties, such as low carrier mobilities, compared to covalent semiconducting compounds. The enhanced Born charges and the resulted large static dielectric constants are more effective in screening the charged impurities and defects,[3] which may be carrier traps and recombination centers. Thus, the significant Born charge enhancement may improve the carrier mobility and lifetime, which are important parameters for the semiconductor radiation detectors.

The carrier transport is also strongly influenced by the defect properties. A combination of the effective dielectric screening and benign electric properties of the defects may result in surprisingly good $\mu\tau$ products. For examples, the $\mu\tau$ products for both electrons and holes in TlBr (Refs. 35–39) are comparable to that in CdTe (in the orders of 10^{-3} cm^2/V for electrons and 10^{-4} cm^2/V for holes) despite the fact that TlBr is a soft-lattice ionic compound, which is usually prone to the defect formation and has a low mobility. This may be explained by the combination of the large static dielectric constant of TlBr (as a result of large Born charges)[3] and the theoretical results that show that the native defects in TlBr do not induce deep electron trapping levels in the band gap.[40]

It should be noted that the reported $\mu\tau$ products for InI,[5,6] PbI_2, and BiI_3 (Refs. 7, 10, and 34) are generally smaller than that of TlBr.[35–39] This points to the need for further defect studies in these materials in order to better understand the transport properties and the performance of these materials as radiation detectors. The $\mu\tau$ products of these materials may improve substantially in the future through better defect and impurity management. But it is possible that the layered structures of InI, PbI_2, and BiI_3 are more prone to the formation of defects as opposed to the simple cubic structure of TlBr. The layered structure also causes anisotropy in phonon scattering and dielectric screening. Among all the halides studied in this paper, indium halides have much stronger interlayer bonding than PbI_2 and BiI_3. Taking InI as an example, the interlayer In-In bond length is 3.57 Å, not much longer than the intralayer In-I bond lengths of 3.25 and 3.46 Å. For comparison, the interlayer I-I distance in PbI_2 is 4.15 Å, substantially longer than the intralayer Pb-I bond length of 3.24 Å. Similarly, the interlayer I-I distance in BiI_3 is about 4.1 Å, also much longer than the intralayer Bi-I bond length of about 3.1 Å. Also, the phonon anisotropy in InI is small as discussed in Sec. III A and consequently the anisotropy in Born charges and static dielectric constant is also small in contrast to PbI_2 and BiI_3.

V. SUMMARY

We have calculated the electronic structure and lattice dynamics of several III-VII, IV-VII_2, and V-VII_3 compounds, many of which have been investigated for potential room-temperature radiation detection applications due to their large atomic numbers, suitable band gaps, and high resistivity. The results show that the Born effective charges of these compounds are substantially larger than the nominal ionic charges, which are consistent with the large LO-TO splitting that we find in these compounds. The common characteristic of these largely ionic compounds is that the outmost cation-s states are occupied, resulting in the CBM states being derived from the spatially more extended cation-p states. This

causes enhanced cross-band-gap hybridization between the cation-*p* and the halogen-*p* states, leading to enhanced Born charges. This is the same mechanism as in many ferroelectric oxides. Here the large Born effective charges provide an explanation of the large static dielectric constants that are observed experimentally in these compounds. The large dielectric constant provides more effective screening of the charged impurities and defects, thereby improving the carrier transport properties, which are important to the semiconductor radiation detectors. This study provides important insights to the performance of radiation detectors based on the soft-lattice semiconductor compounds with enhanced Born effective charges.

ACKNOWLEDGMENTS

This work was supported by the U.S. DOE Office of Nonproliferation Research and Development NA22.

[1] S.-H. Wei and A. Zunger, Phys. Rev. B **55**, 13605 (1997).
[2] M. Schreiber and W. Schäfer, Phys. Rev. B **29**, 2246 (1984).
[3] M.-H. Du and D. J. Singh, Phys. Rev. B **81**, 144114 (2010).
[4] Ph. Ghosez, J.-P. Michenaud, and X. Gonze, Phys. Rev. B **58**, 6224 (1998).
[5] P. Bhattacharya, M. Groza, Y. Cui, D. Caudel, T. Wrenn, A. Nwankwo, A. Burger, G. Slack, and A. G. Ostrogorsky, J. Cryst. Growth **312**, 1228 (2010).
[6] T. Onodera, K. Hitomi, and T. Shoji, IEEE Trans. Nucl. Sci. **53**, 3055 (2006).
[7] K. S. Shah, F. Olschner, L. P. Moy, P. Bennett, M. Misra, J. Zhang, M. R. Squillante, and J. C. Lund, Nucl. Instrum. Methods Phys. Res. A **380**, 266 (1996).
[8] X. H. Zhu, Z. R. Wei, Y. R. Jin, and A. P. Xiang, Cryst. Res. Technol. **42**, 456 (2007).
[9] M. Matuchova, K. Zdansky, and J. Zavadil, Mater. Sci. Eng., B **165**, 60 (2009).
[10] A. T. Lintereur, W. Qiu, J. C. Nino, and J. E. Baciak, Proc. SPIE **6945**, 694503 (2008).
[11] G. E. Jellison, J. O. Ramey, and L. A. Boatner, Phys. Rev. B **59**, 9718 (1999).
[12] G. Kresse and D. Joubert, Phys. Rev. B **59**, 1758 (1999).
[13] P. Giannozzi *et al.*, J. Phys.: Condens. Matter **21**, 395502 (2009).
[14] J. P. Perdew, K. Burke, and M. Ernzerhof, Phys. Rev. Lett. **77**, 3865 (1996).
[15] T. Staffel, and G. Meyer, Z. Anorg. Allg. Chem. **552**, 113 (1987).
[16] G. Meyer and T. Staffel, Z. Anorg. Allg. Chem. **574**, 114 (1989).
[17] C. P. J. M. van der Vorst, G. C. Verschoor, and W. J. A. Maaskant, Acta Crystallogr., Sect. B: Struct. Crystallogr. Cryst. Chem. **34**, 3333 (1978).
[18] M. I. Kolinko, J. Phys.: Condens. Matter **6**, 183 (1994).
[19] M. I. Kolinko, Phys. Rev. B **55**, 4007 (1997).
[20] M. Yoshida, N. Ohno, and H. Watanabe, J. Phys. Soc. Jpn. **53**, 408 (1984).
[21] N. Ohno, M. Fujita, Y. Nakai, and K. Nakamura, Solid State Commun. **28**, 137 (1978).
[22] M. Yoshida, N. Ohno, K. Nakamura, and Y. Nakai, Phys. Status Solidi B **109**, 503 (1982).
[23] R. E. Cohen, Nature (London) **358**, 136 (1992).
[24] W. Zhong, R. D. King-Smith, and D. Vanderbilt, Phys. Rev. Lett. **72**, 3618 (1994).
[25] M. Posternak, R. Resta, and A. Baldereschi, Phys. Rev. B **50**, 8911 (1994).
[26] B. P. Clayman, R. J. Nemanich, J. C. Mikkelsen, Jr., and G. Lucovsky, Phys. Rev. B **26**, 2011 (1982).
[27] N. Ohno, M. Yoshida, K. Nakamura, and Y. Nakai, J. Phys. Soc. Jpn. **49**, 1391 (1980).
[28] B. Palosz and W. Steurer, and H. Schulz, J. Phys.: Condens. Matter **2**, 5285 (1990).
[29] L. Keller and D. Nason, Powder Diffr. **11**, 91 (1996).
[30] G. Lucovsky, R. M. White, W. Y. Liang, R. Zallen, and Ph. Schmid, Solid State Commun. **18**, 811 (1976).
[31] A. E. Dugan and H. K. Henisch, J. Phys. Chem. Solids **28**, 971 (1967).
[32] P. Vits, Diplomarbeit, RWTH Aachen, 1973.
[33] R. Clasen, Thesis, RWTH Aachen, 1974.
[34] A. Owens and A. Peacock, Nucl. Instrum. Methods Phys. Res. A **531**, 18 (2004).
[35] A. V. Churilov, G. Ciampi, H. Kim, L. J. Cirignano, W. M. Higgins, F. Olschner, and K. S. Shah, IEEE Trans. Nucl. Sci. **56**, 1875 (2009).
[36] H. Kim, L. Cirignano, A. Churilov, G. Ciampi, W. Higgins, F. Olschner, and K. Shah, IEEE Trans. Nucl. Sci. **56**, 819 (2009).
[37] M. Shorohov, M. Kouznetsov, I. Lisitskiy, V. Ivanov, V. Gostilo, and A. Owen, IEEE Trans. Nucl. Sci. **56**, 1855 (2009).
[38] T. Onodera, K. Hitomi, T. Shoji, Y. Hiratate, and H. Kitaguchi, IEEE Trans. Nucl. Sci. **52**, 1999 (2005).
[39] K. Hitomi, T. Onodera, and T. Shoji, Nucl. Instrum. Methods Phys. Res. A **579**, 153 (2007).
[40] Mao-Hua Du (unpublished).